

arrakis

THERAPEUTICS

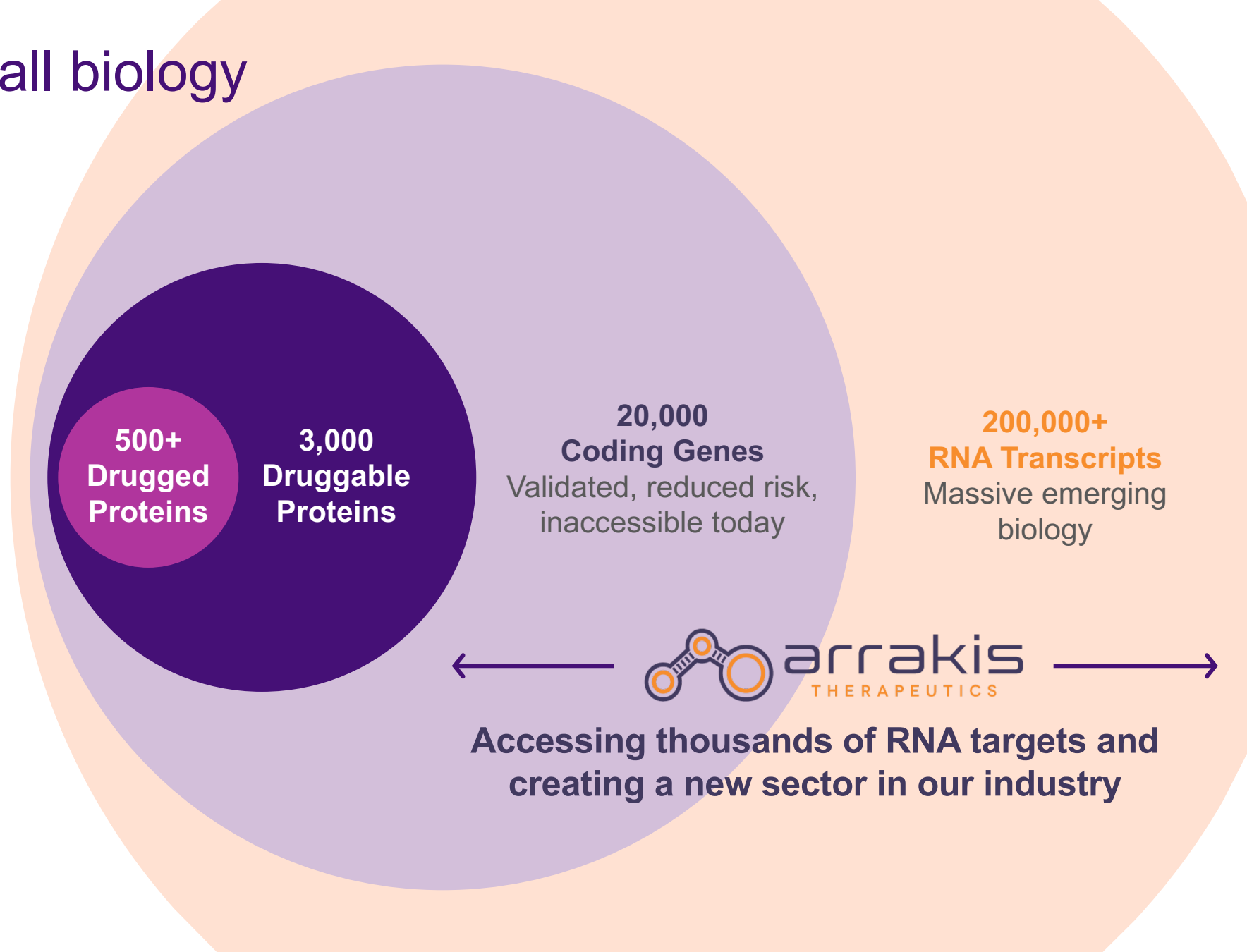
**A STRUCTURE-BASED APPROACH TO
DRUGGING RNA WITH SMALL MOLECULES**

Cell Symposium: Chemical Biology in Drugging the Undrugged

JENNIFER PETTER | 4 DECEMBER 2024

RNA is upstream of all biology

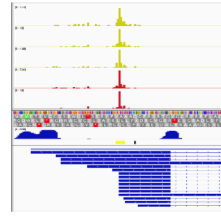
- Our goal is to unlock this previously inaccessible therapeutic target space by developing drug-like small molecule ligands for RNA (rSMs).
- This requires building a toolkit for RNA drug discovery.



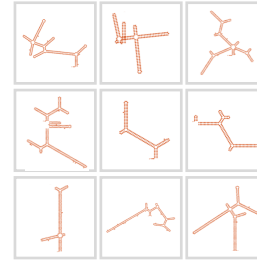
Comprehensive platform for target identification, rSM lead discovery, and optimization

1

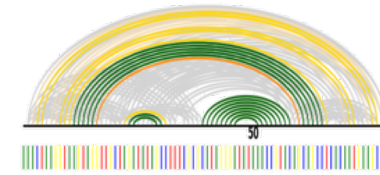
Target ID and structure prediction



transcriptomic analysis



RNA structures in cells



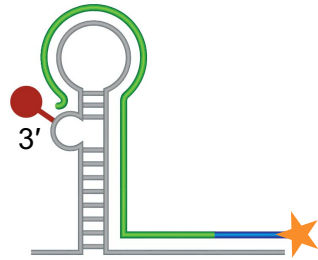
RNA structure modeling



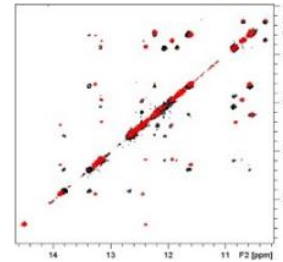
synthetic RNAs

2

Structure confirmation and rSM ID



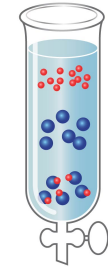
chemical probing



3D structures by NMR



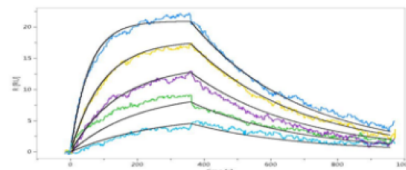
3D structures by SAXS



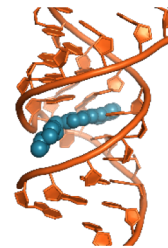
HTS via SEC-MS

3

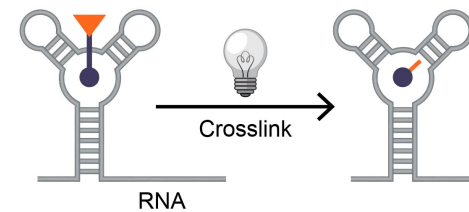
rSM characterization and optimization



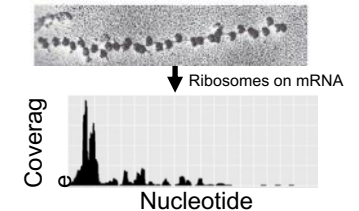
biophysical methods



rSM-RNA crystal structures



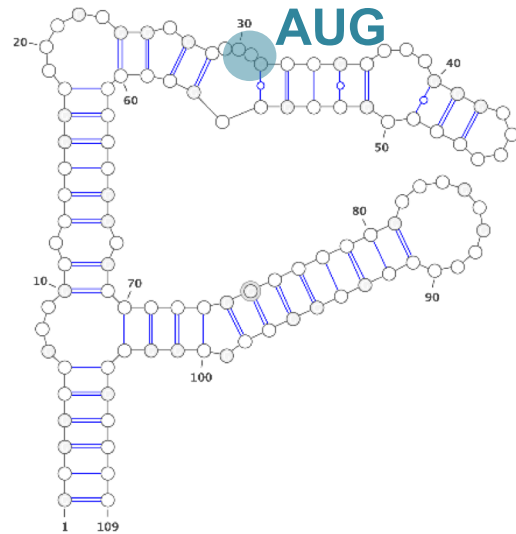
target engagement



translation impact

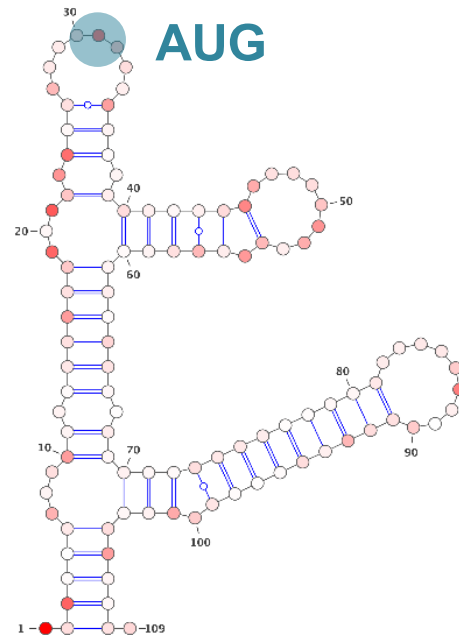
The folding of mRNA structures can be recapitulated *in vitro*

Naïve *in silico* prediction



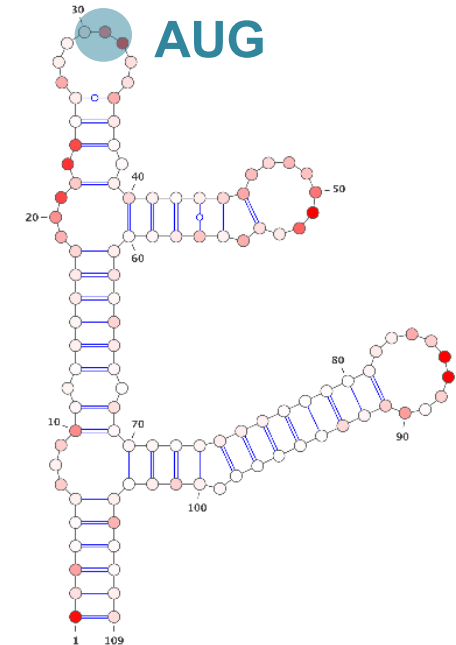
Vienna RNA fold

In-cell mRNA structure with SHAPE data incorporated

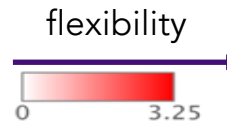


Translation sub-target fold in context of entire mRNA, from HepG2 cells

In vitro RNA structure



In vitro screening construct folding is similar to in-cell structure



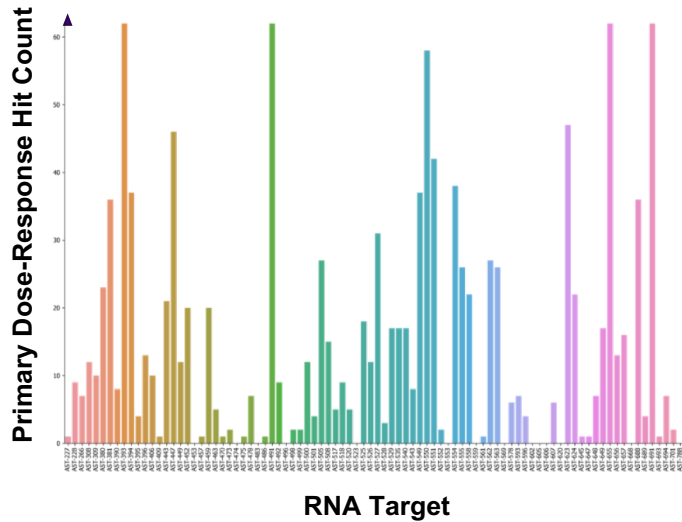
SEC-MS identifies druglike, structurally diverse, selective rSMs

RNA screening is successful

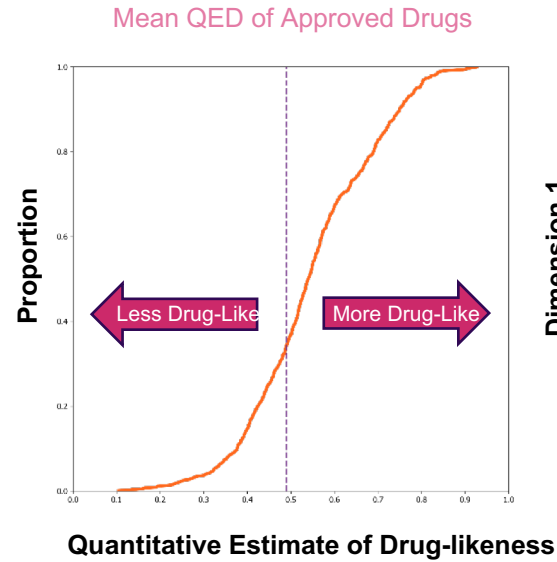
Hits are drug-like...

...structurally diverse

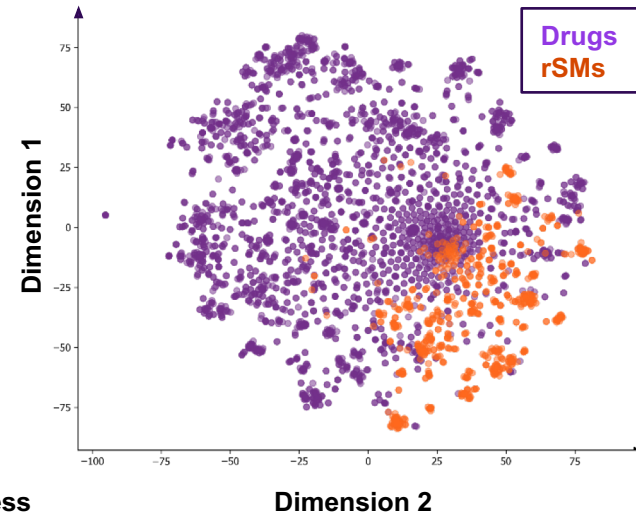
...and selective



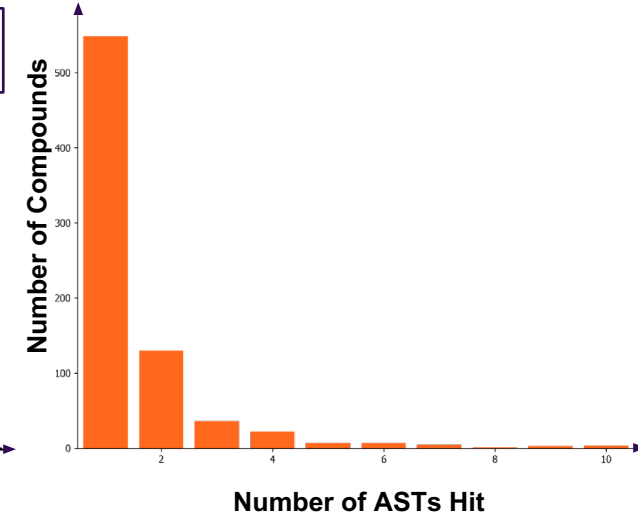
ca. 84% of screens yield confirmed hits



Most confirmed hits are predicted to be drug-like

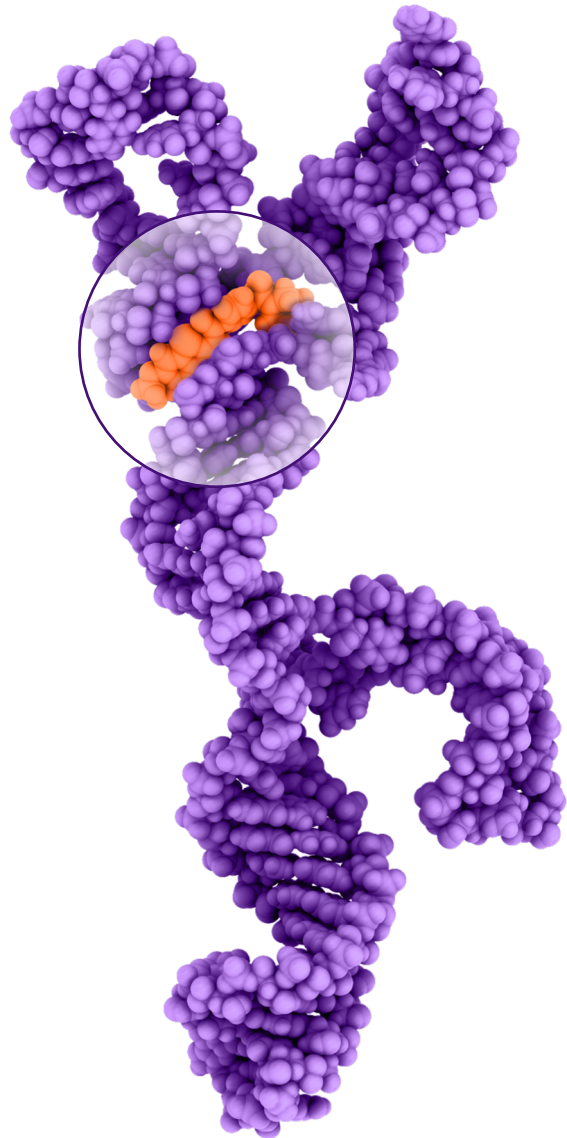


Confirmed hits occupy a sub-space spanned by drugs



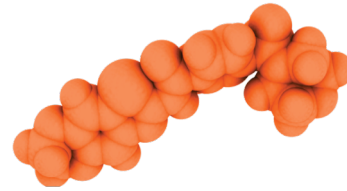
88% of confirmed hits bind to fewer than 3 ASTs

Multiple therapeutic rSM modalities



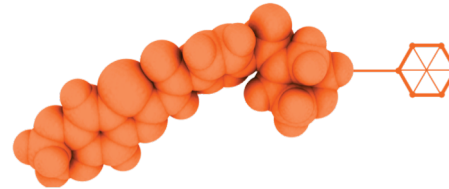
rSM FUNCTION

INTRINSIC



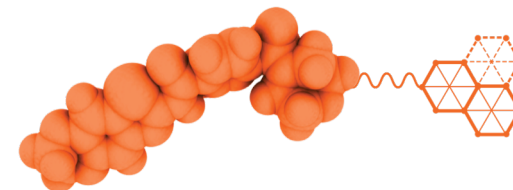
Ligand modulates RNA function by modifying structure

COVALENT



Forms adduct to permanently block target RNA function

PROXIMITY



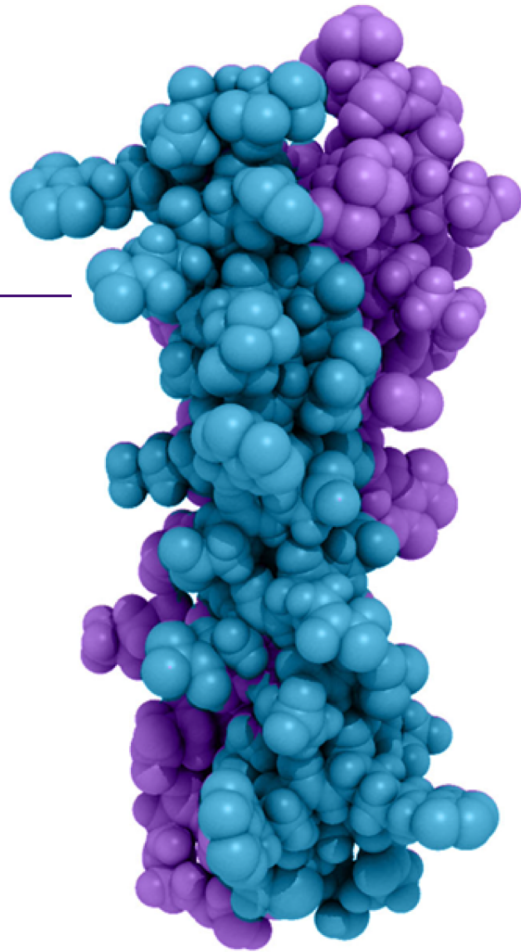
Recruits host effector, or sequesters RNA for specific biological function on target RNA

MYC, a holy grail oncology target

Protein

Lacks druggable binding pockets

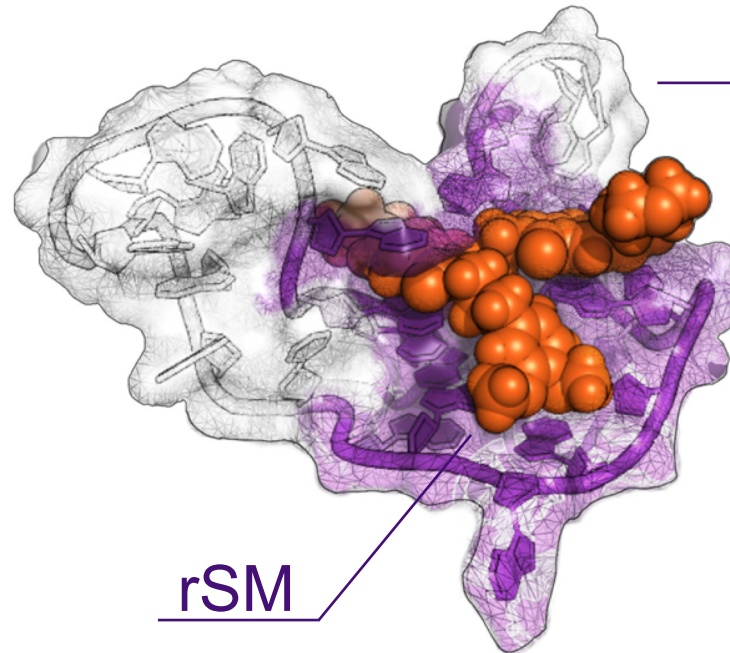
Multiple efforts to drug the MYC protein have failed



mRNA

Multiple ligandable structures identified in MYC mRNA

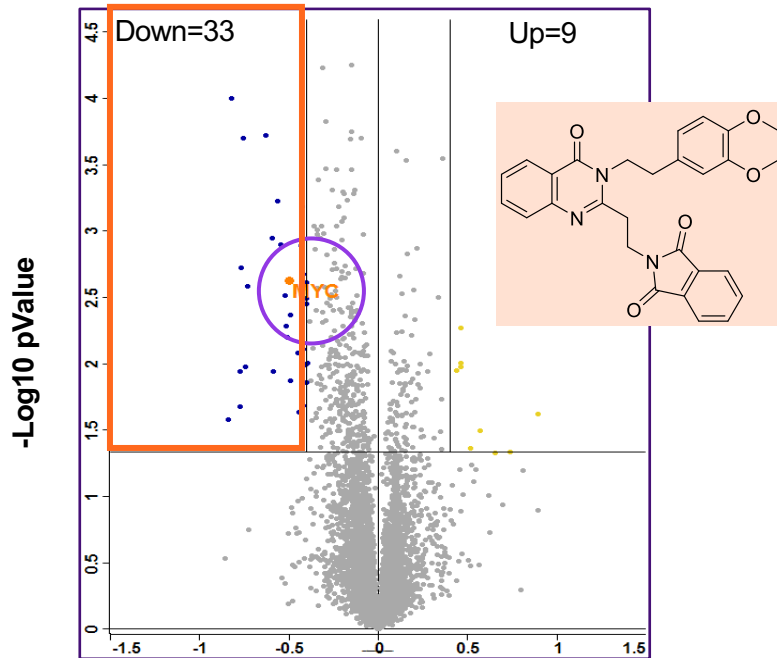
Arrakis has identified ligands across conserved 5'-UTR



Orally available RNAi mimic that selectively inhibits MYC

Inhibition of MYC translation with small molecules with potential to penetrate tumors

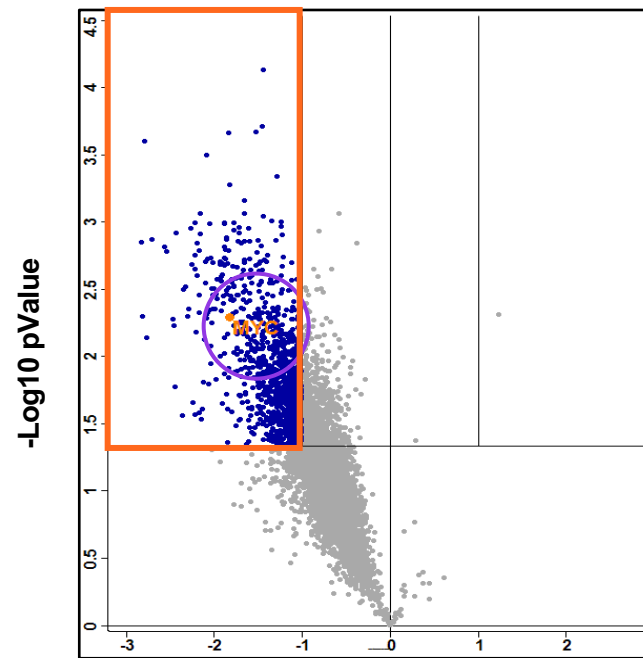
ARK-84291 selectively decreases MYC protein levels



Heavy Protein Log2 Fold Change
ARK-Compound / DMSO

10 μM ARK-Compound vs. DMSO

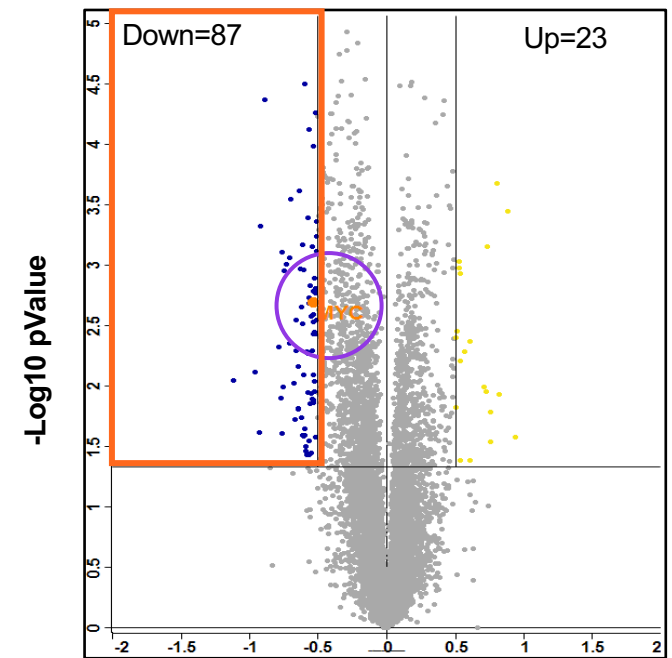
unlike rocaglamide A



Heavy Protein Log2 Fold Change
RocA / DMSO

300 nM RocA vs. DMSO

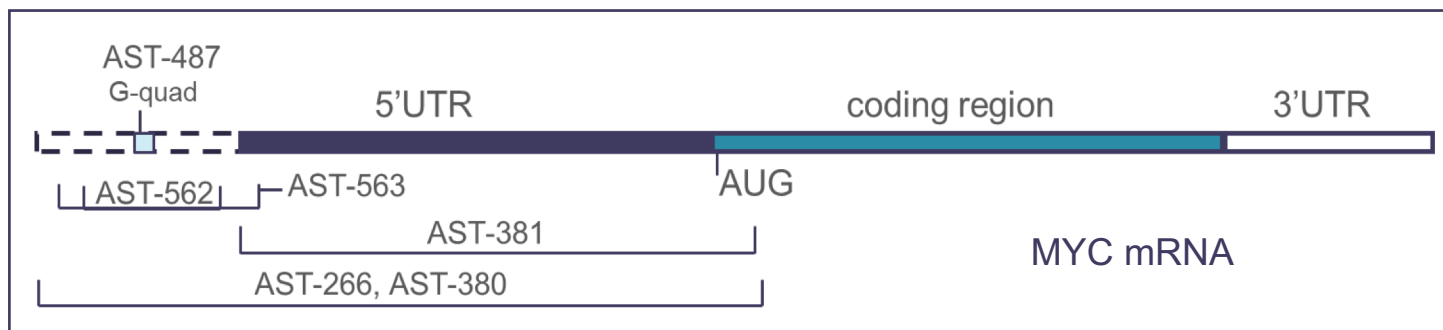
but similar to siRNA



Heavy Protein Log2 Fold Change
siMYC / siNTC

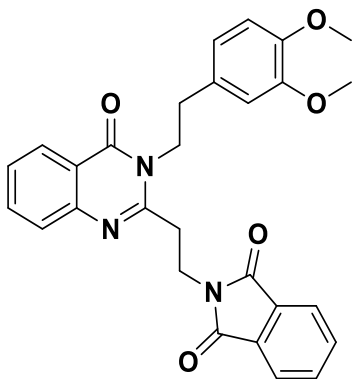
48h siMYC vs. 48h siNTC

ARK-84291 shows selective binding to long MYC isoforms

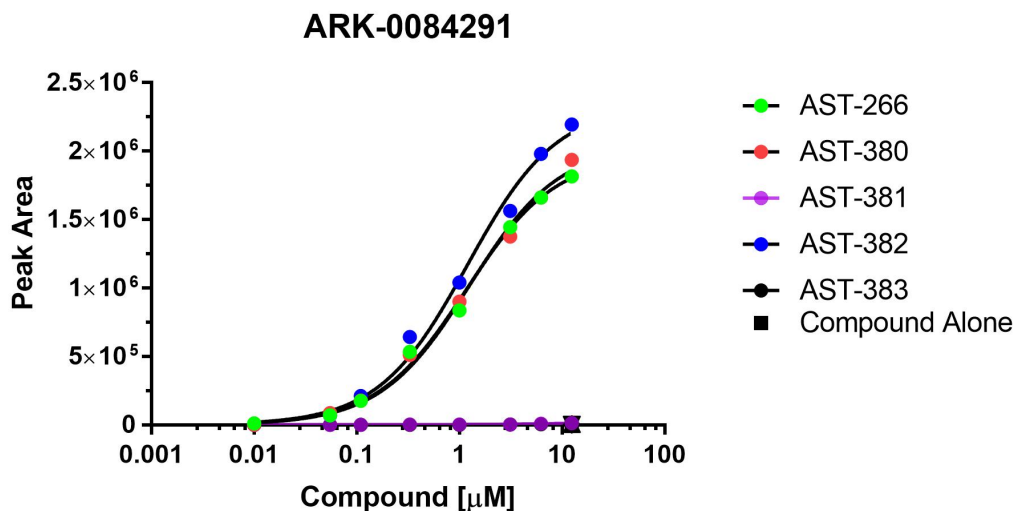


- ARK-84291 identified by SEC-MS screening of internal drug-like library
- ARK-84291 binds ($K_D(\text{app}) \sim 1.2 \mu\text{M}$) RG4-containing 'long' constructs
- ARK-84291 does not bind to the 'short' constructs with no RG4
- Binding confirmed via SPR, DSF, and NMR

SEC-MS binding data



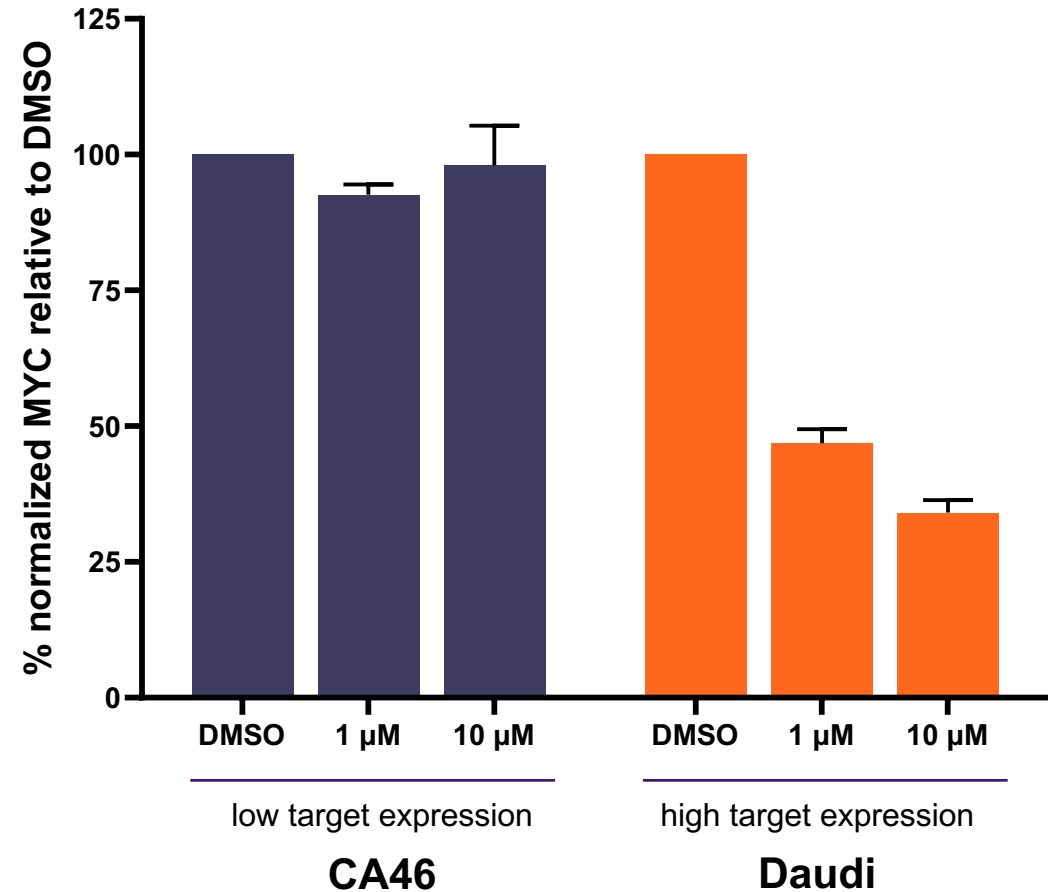
ARK-84291



AST	$K_D(\text{app}) \mu\text{M}$	MYC isoform
266	1.2	Long
380	1.3	Long
382	1.2	Long
381	> 12	Short
383	> 12	Short

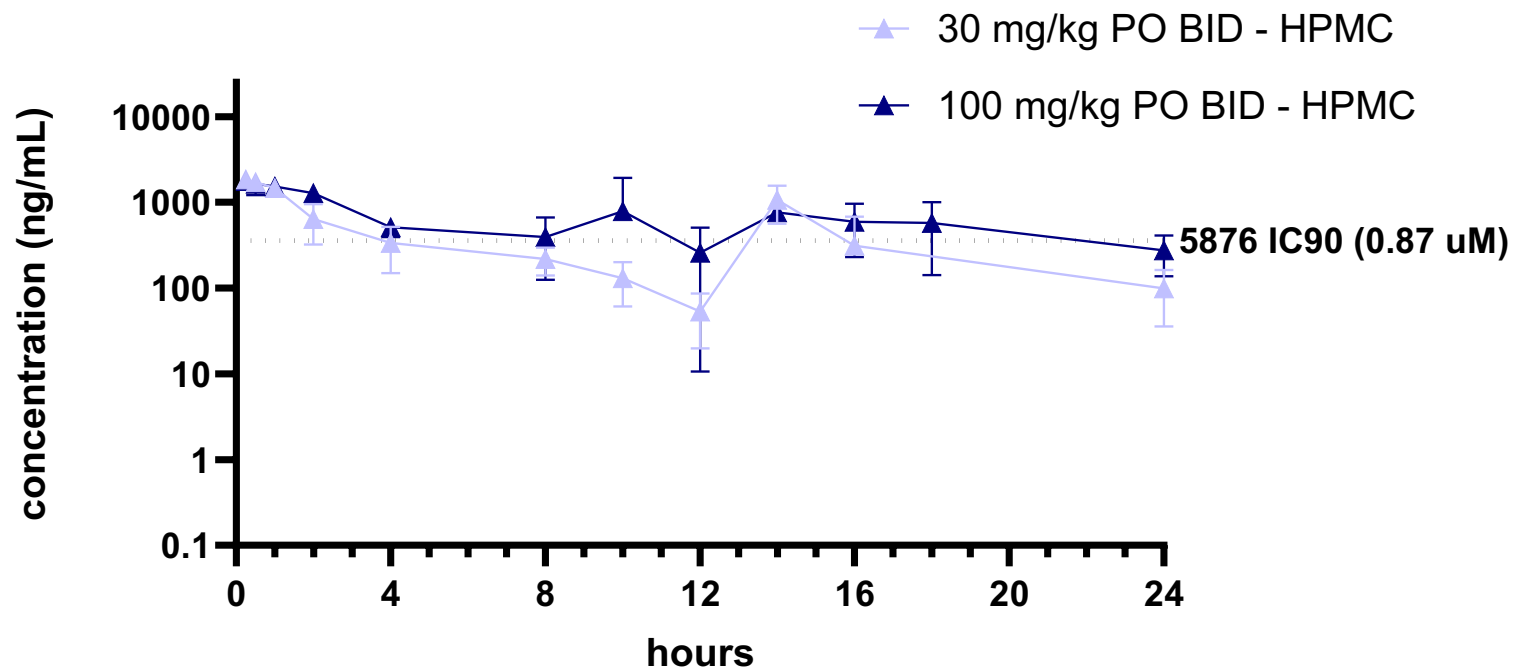
ARK-84291 selectively inhibits MYC expression in cell lines that rely on the upstream promoter

ARK-84291 only affects MYC protein levels in Daudi cancer cells expressing long-form MYC



ARK-175876 PO BID dosing

ARK175876 BID HPMC PK



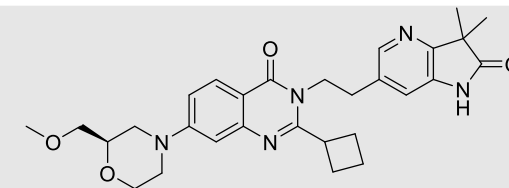
Oral Formulation: 0.5 % HPMC and 0.2% tween 80 (suspension)

Adverse events: No adverse events

30 mpk used Batch 001

100 mpk used Batch 002

ARK-0175876

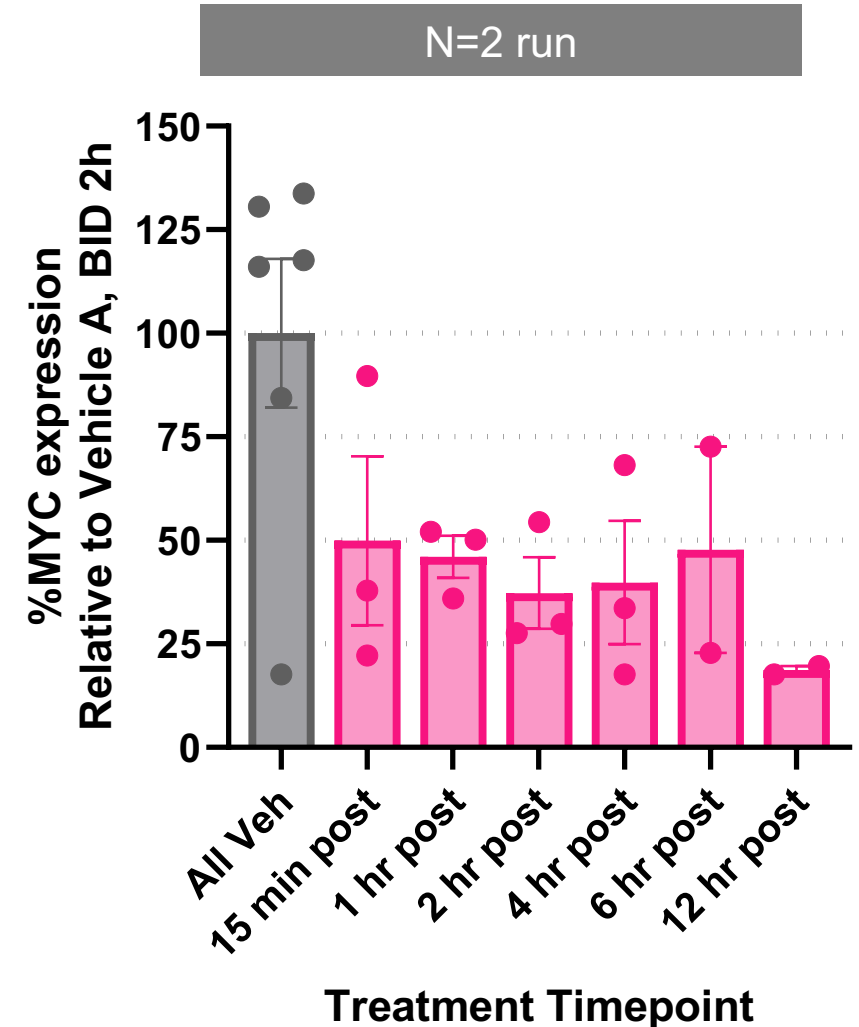
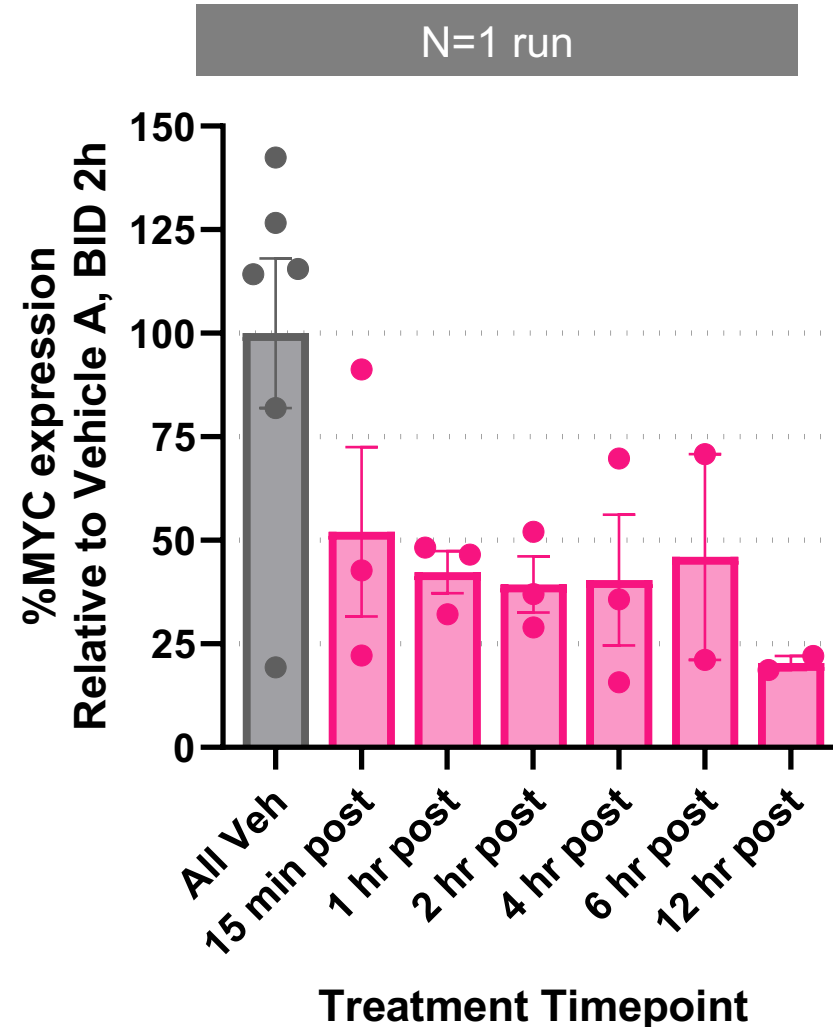


LogD, TPSA	3.2, 98.6
Kinetic Sol (μM): PBS Buffer	67
PAMPA, P_{app} (cm/s)	7.9×10^{-6}
MDCKII-MDR1 P_{app} (A-B) (10^{-6} cm/s) / ER	5.0 / 7
MLM CL_{int} (uL/min/mg)	73
HLM CL_{int} (uL/min/mg)	164
PPB % Unbound (Mouse / Human)	2 / 3.3
MYC Hibit (IC_{50}) (μM) / IC_{90} (μM)	0.083 / 0.693

PK parameters	30 mg/kg PO BID HPMC	100 mg/kg PO BID HPMC
$T_{1/2}$ (h)	N/A	N/A
T_{max} (h)	0.33	0.33
C_{max} (ng/mL)	1887 (3.6 μM)	1807 (3.4 μM)
AUC_{last} (h*ng/mL)	9282	14776
AUC_{Inf} (h*ng/mL)	N/A	N/A
F (%)	N/A	N/A
Cl_{obs} (mL/min/kg)	27	27
$V_{\text{ss_obs}}$ (L/kg)	0.94	0.94

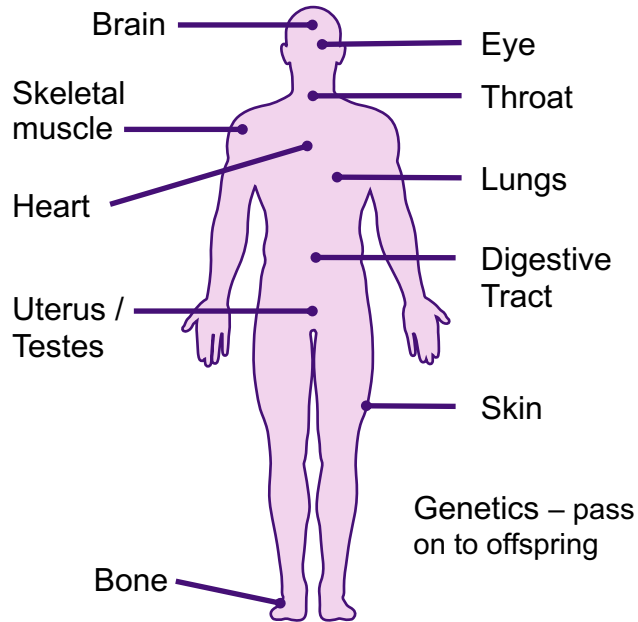
MYC knockdown by ARK-175876 in xenografts

- ARK-175876 was administered to mice in a Daudi xenograft model at 100 mg/Kg PO BID
- MYC protein expression showed up to 50% MYC reduction in xenograft cells
- Knockdown was measured out to 12 hours post-2nd dose



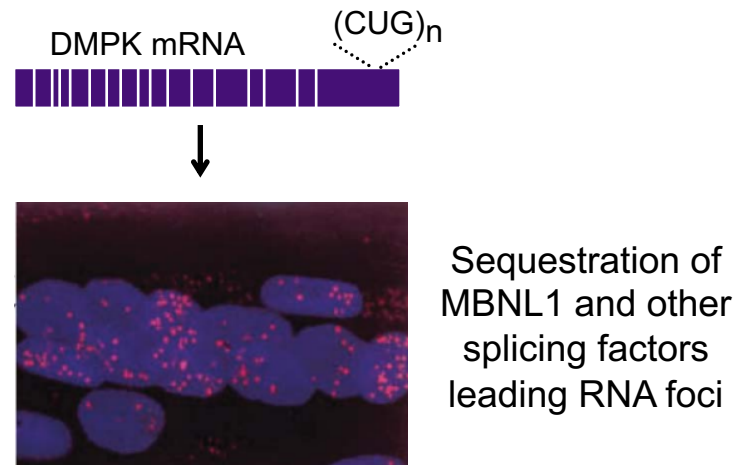
Myotonic dystrophy type 1 (DM1) is a repeat expansion disease for which the RNA is pathogenic

DM1 is a multi-system disease



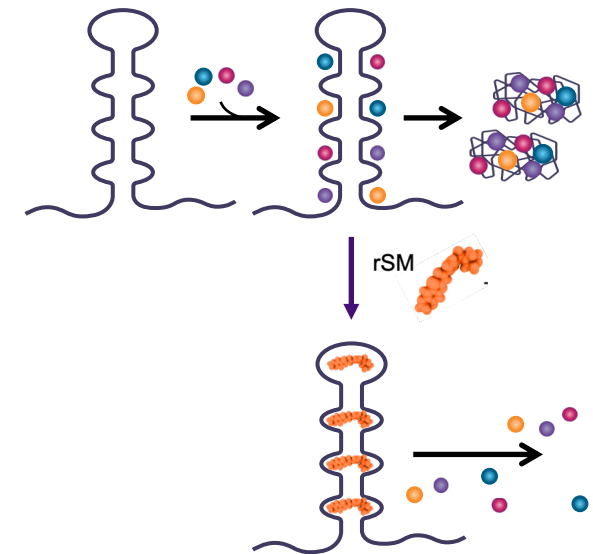
- Effects ~1:8000 WW
- Symptoms include myotonia, muscle wasting, cataracts, and cardiac conduction abnormalities

Caused by a pathogenic mRNA expansion repeat



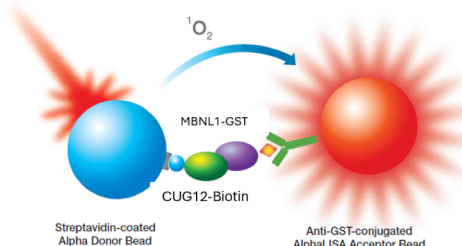
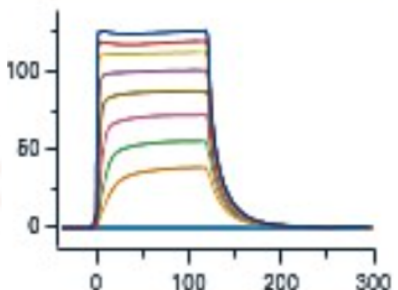
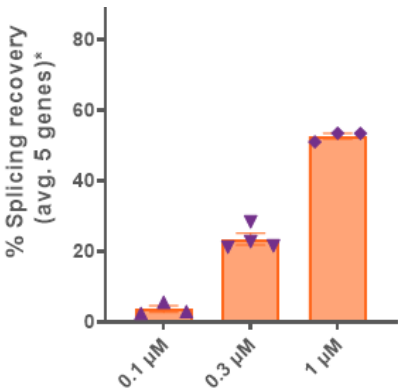
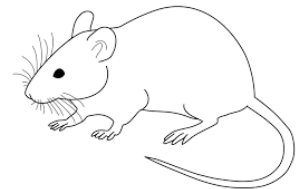
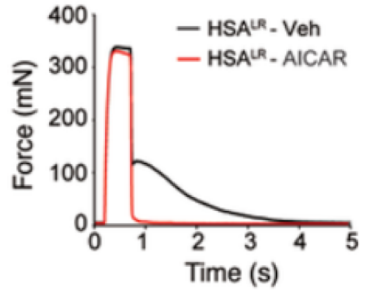
- Mis-splicing of >100 target genes
- Current therapeutics are unlikely to address the full disease manifestations beyond muscle

rSMs can bind and liberate bound MBNL1



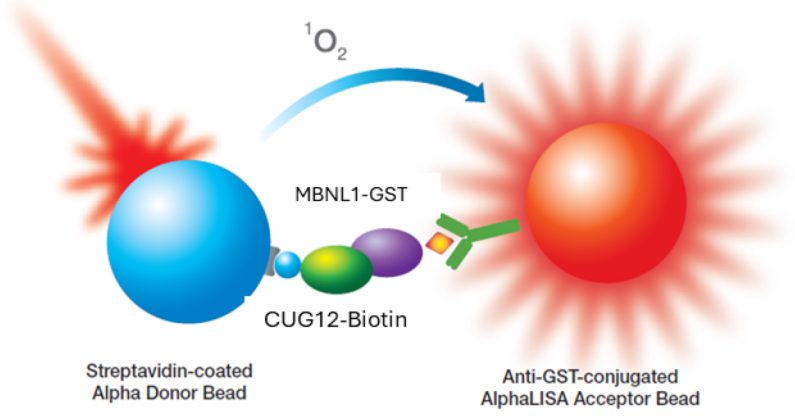
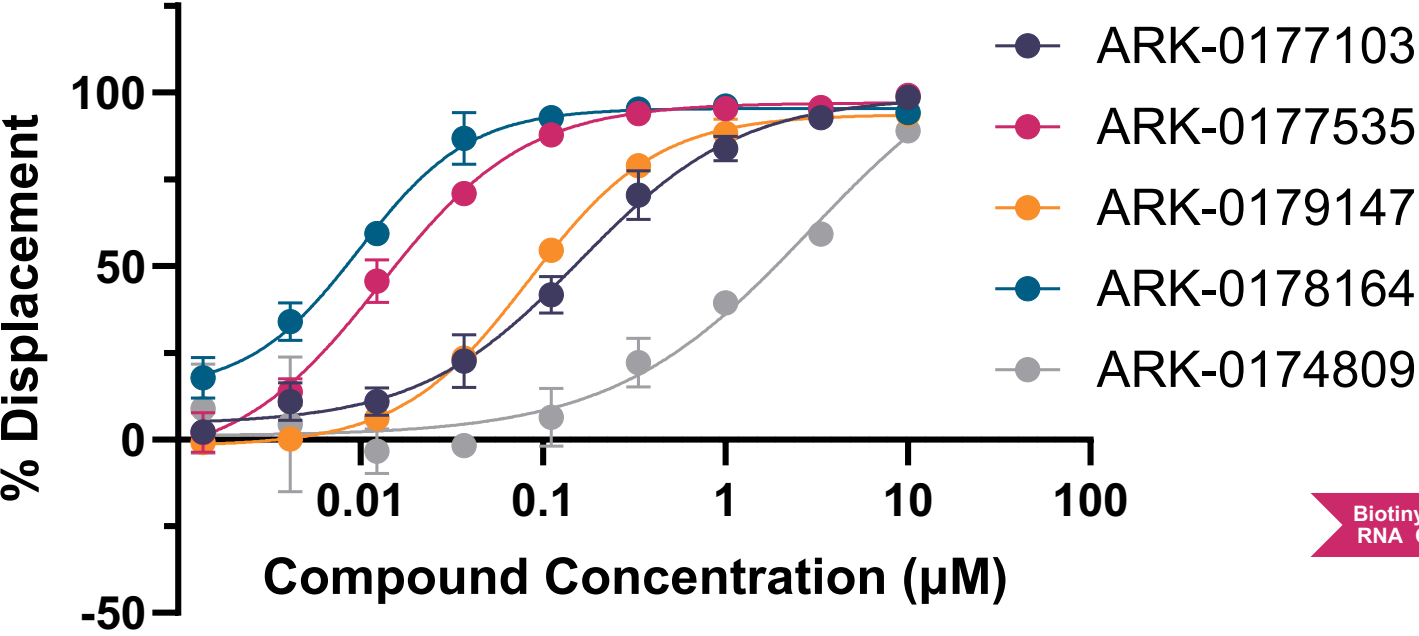
- Arrakis has identified multiple ligands in two distinct chemical series that bind CUG pathologic RNA and displace key RNA splicing factors

DM1 program assays

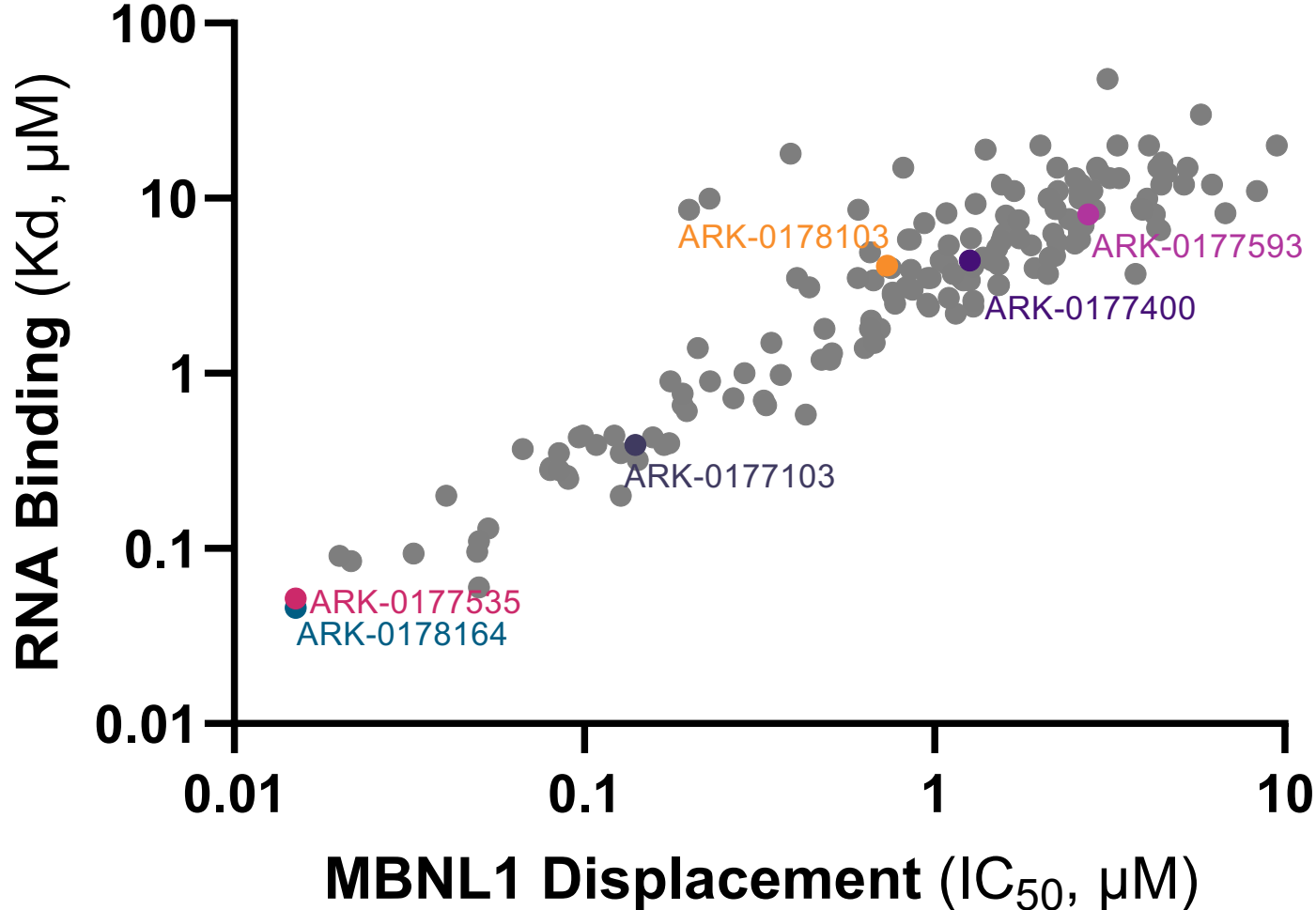
	MBNL1 Displacement	Binding by SPR	Cellular Activity	PD	Efficacy
Readout	Displacement of MBNL1 from r(CUG) ₁₂ (AlphaScreen)	r(CUG) ₁₂ binding to cpd (SPR)	Splicing rescue in patient-derived myocytes/tubes	Splicing rescue in HSA ^{LR} mouse muscle	Muscle relaxation time
		 <p>Ch 4; ARK-0177103-001;</p>			 <p><i>Example relaxation curve</i></p>
Throughput	Up to 2000/month	Up to 200/month	Up to 80/month	Up 10/month*	Up to 8/month*

* Assuming one dose per compound

rSMs displace MBNL1 protein from CUG repeat in a concentration-dependent manner



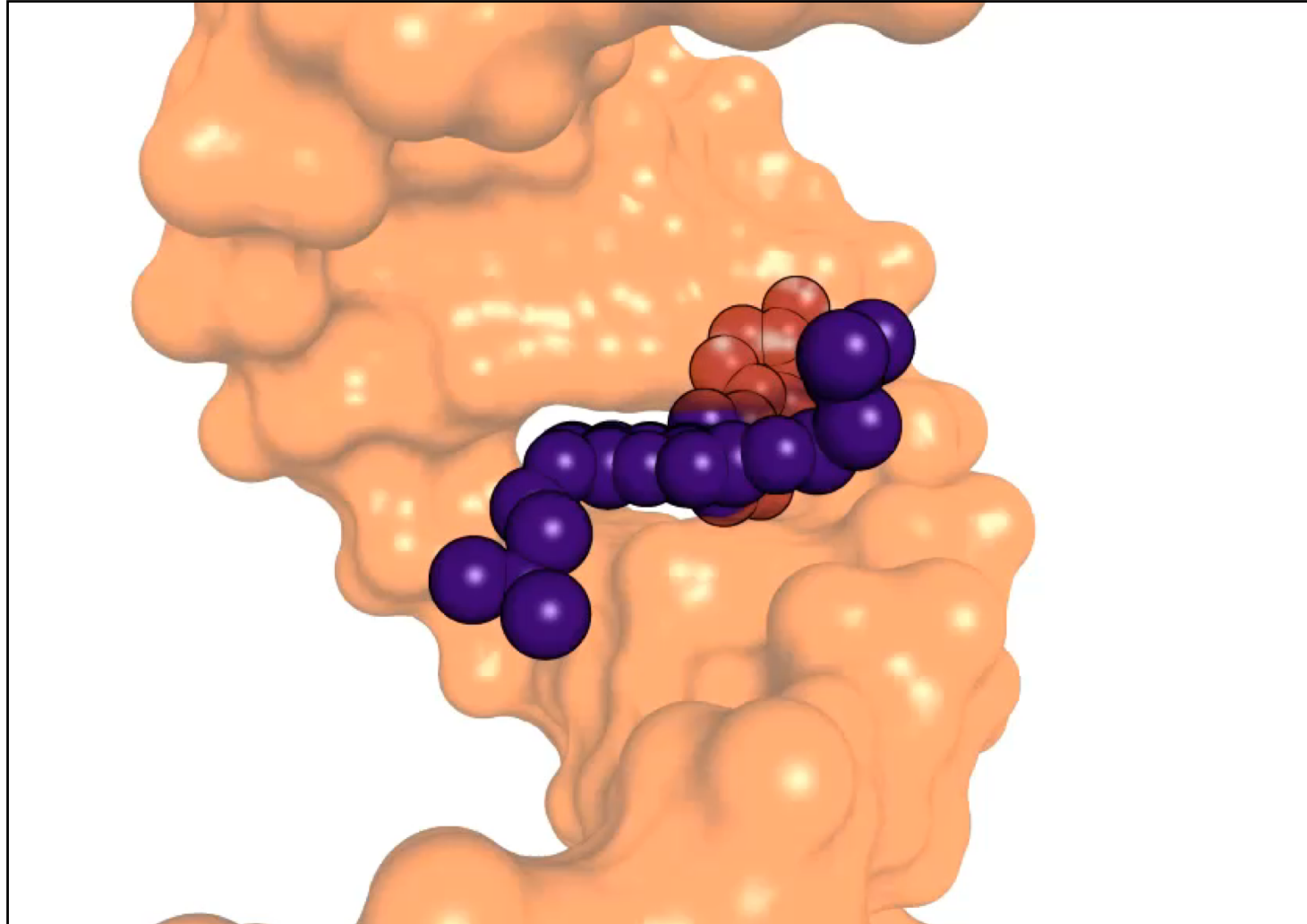
rSMs in two chemical series show correlation between RNA binding and MBNL1 displacement over three logs of potency



Lead compound exhibits selectivity for CUG over other RNA repeats and CTG (DNA)

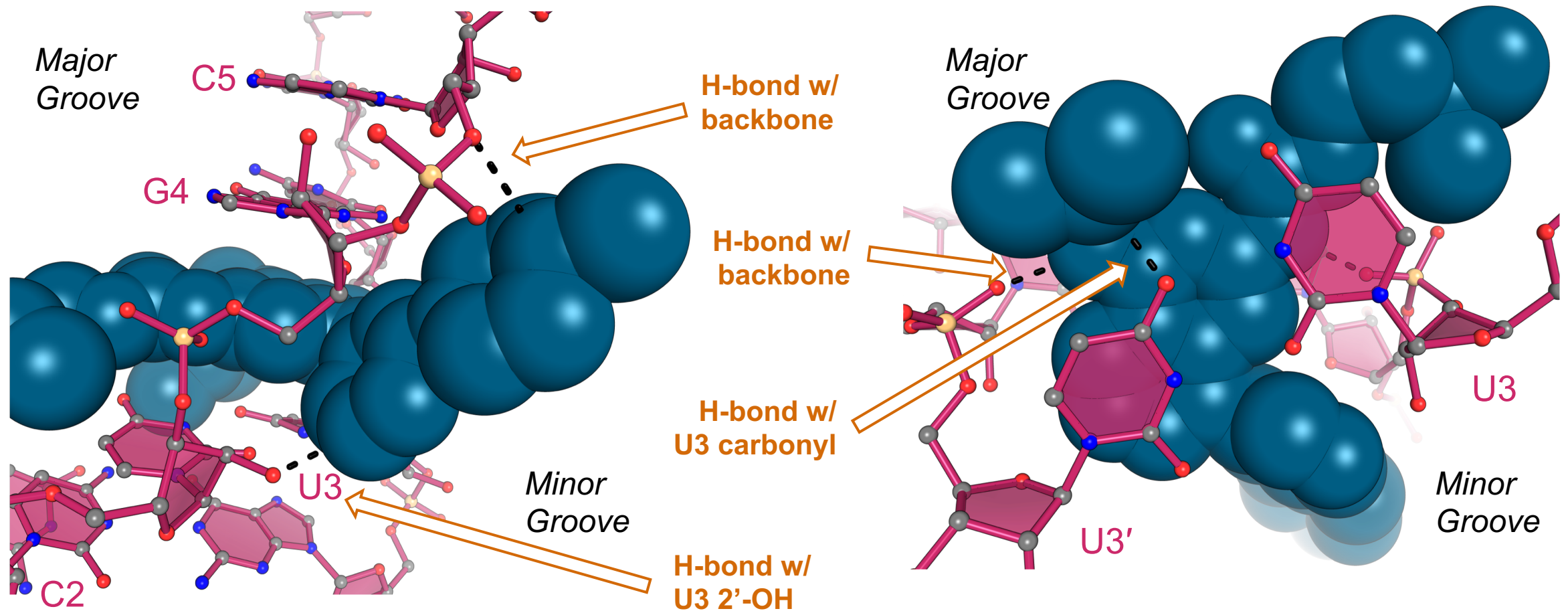
RNA Class	Measurement	ARK-174809	ARK-177103	ARK-177535
CCG RNA	$K_{D, \text{CUG RNA}}$ (nM)	4,910	507	51
CCG RNA	$K_{D, \text{CCG RNA}}$ (nM)	>10,000	13,000	>2,000
CCG RNA	$K_{D, \text{CCG RNA}}/K_{D, \text{CUG RNA}}$	2	25.6	39.2
AUUCU (AST-838)	$K_{D, \text{CUG RNA}}$ (nM)	4,910	507	51
AUUCU (AST-838)	$K_{D, \text{AUUCU RNA}}$ (nM)	>10,000	>20,000	no binding
AUUCU (AST-838)	$K_{D, \text{AUUCU RNA}}/K_{D, \text{CUG RNA}}$	2	39.4	na
GGCCUG (AST-839)	$K_{D, \text{CUG RNA}}$ (nM)	4,910	507	51
GGCCUG (AST-839)	$K_{D, \text{GGCCUG RNA}}$ (nM)	>10,000	>20,000	no binding
GGCCUG (AST-839)	$K_{D, \text{GGCCUG RNA}}/K_{D, \text{CUG RNA}}$	2	39.4	na
AST-452, SL	$K_{D, \text{CUG RNA}}$ (nM)	4,910	507	51
AST-452, SL	$K_{D, \text{AST-452 SL RNA}}$ (nM)	>9,290	4,110	778
AST-452, SL	$K_{D, \text{AST-452 SL}}/K_{D, \text{CUG RNA}}$	>1.9	8.1	15.3
AST-535, 3WJ	$K_{D, \text{CUG RNA}}$ (nM)	4,910	507	51
AST-535, 3WJ	$K_{D, \text{AST-535 3WJ RNA}}$ (nM)	7,250	5,550	1,180
AST-535, 3WJ	$K_{D, \text{AST-535 3WJ}}/K_{D, \text{CUG RNA}}$	1.5	10.9	23.1
RNA vs DNA	$K_{D, \text{CUG RNA}}$ (nM)	4,910	507	51
RNA vs DNA	$K_{D, \text{CTG DNA}}$ (nM)	1,580	2,200	795
RNA vs DNA	$K_{D, \text{CTG DNA}}/K_{D, \text{CUG RNA}}$	0.3	4.4	15.6

X-ray structure (2.8 Å) of rSM bound to CUG RNA repeat



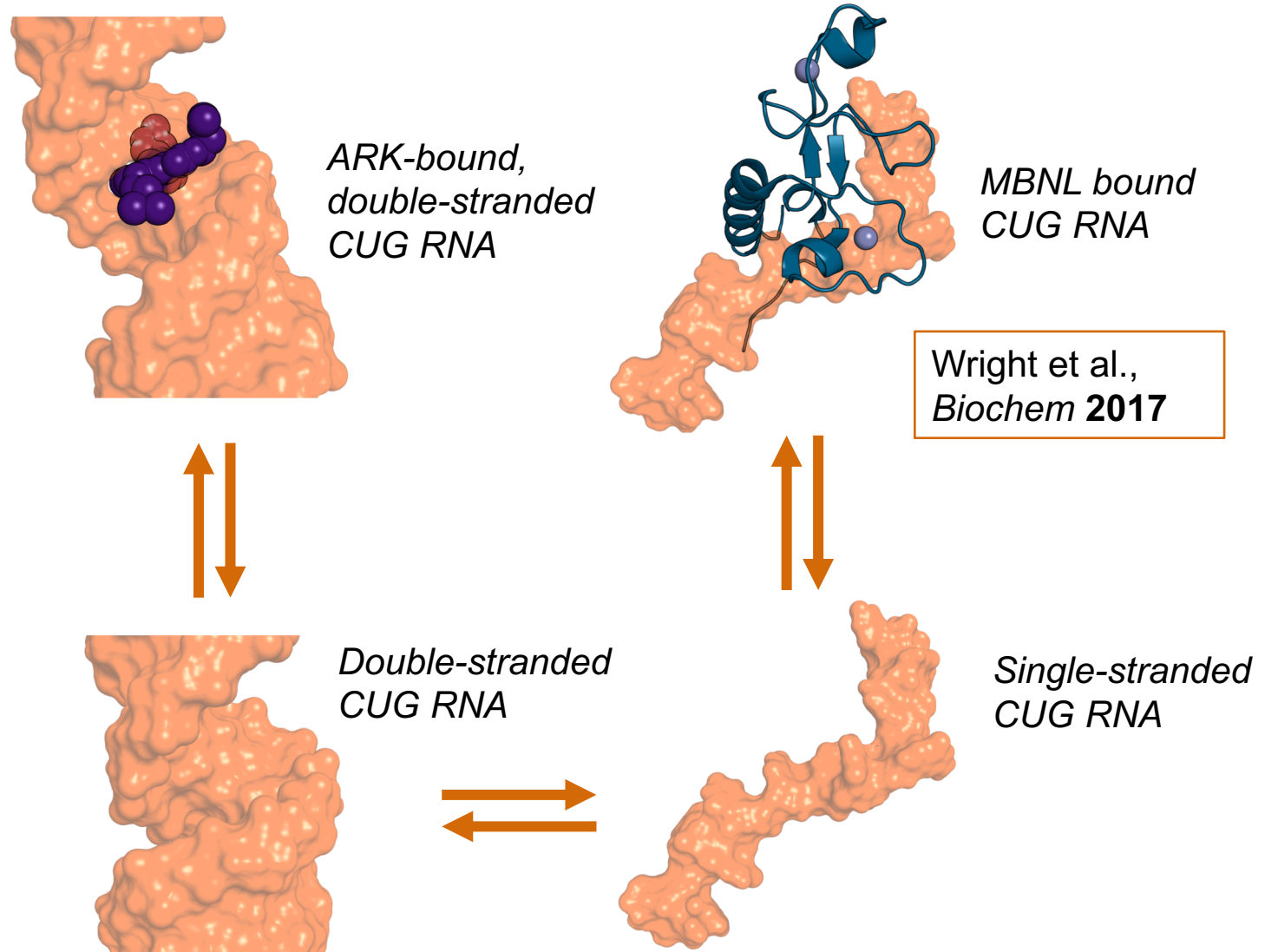
Structure reveals key molecular interactions, informs SAR

- ARK-177535 stacks with a U•U mismatch pair, a recurring feature of CUG repeat RNA structures
- The sidechains form H-bonds with phosphate backbone and 2'OH, contributing to affinity and specificity

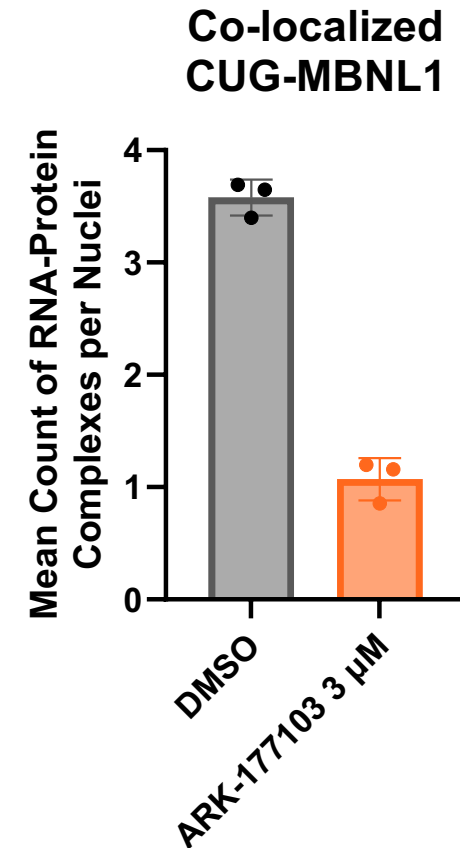
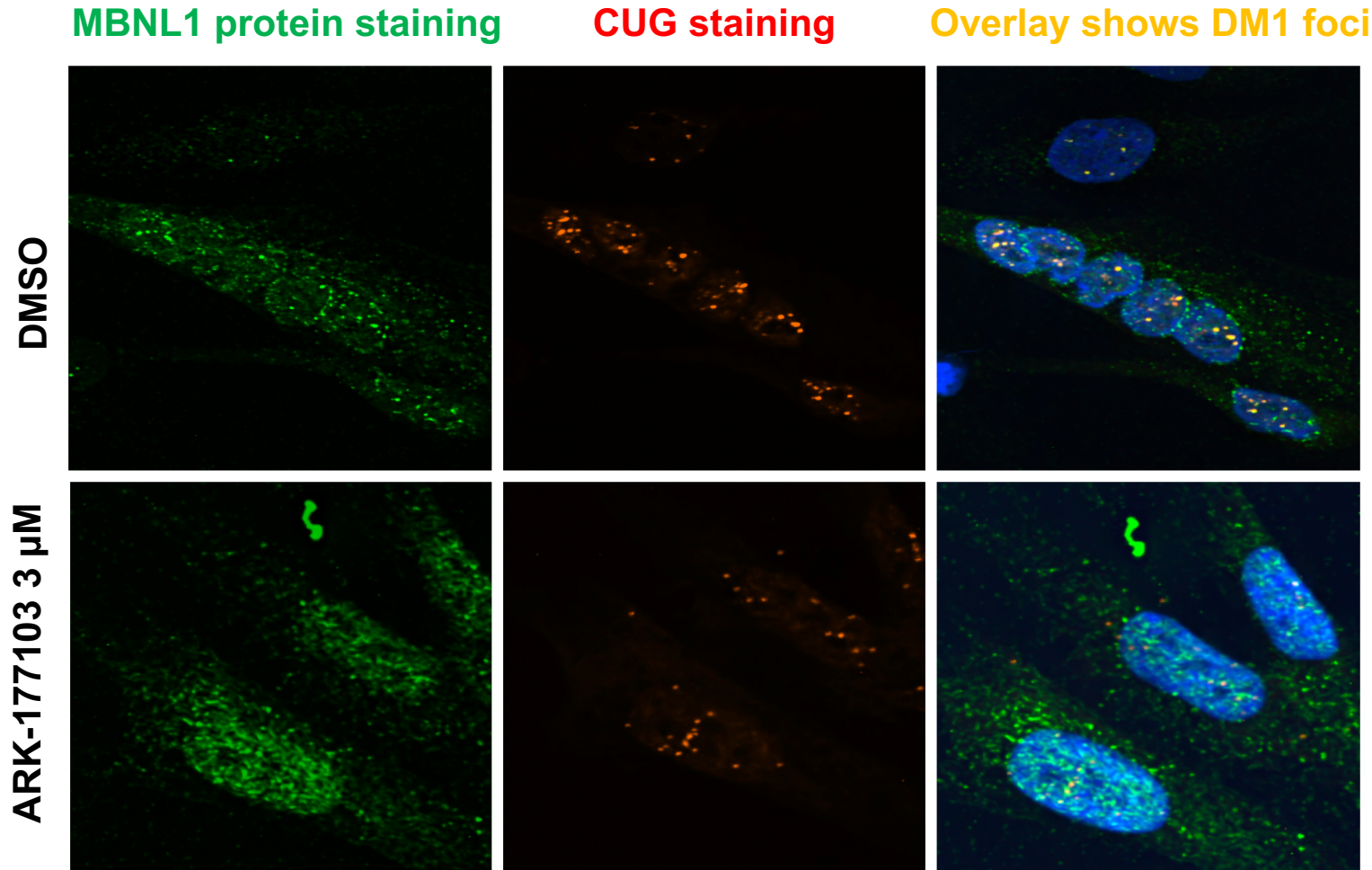


Model for displacement mechanism

- The structure of MBNL complexed with RNA has been solved (both X-ray and NMR)
- Conformation of ligand-bound RNA is quite distinct from the conformation of MBNL-bound RNA
- In light of this, a direct, associative displacement mechanism is unlikely
- Dissociative displacement allows low-energy rearrangement of unbound RNA



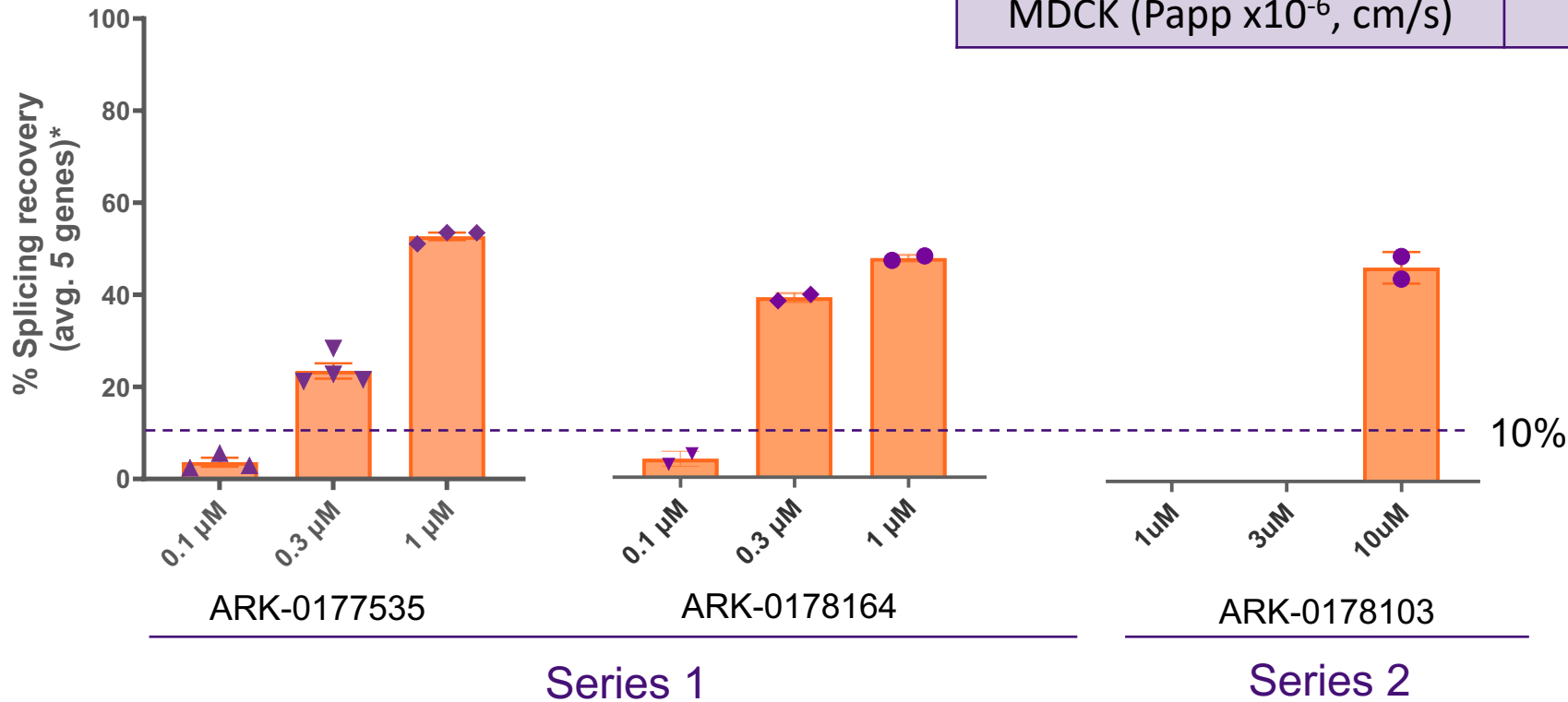
rSM impacts the formation of pathogenic foci in DM1 patient-derived muscle cells



DM1 affected myoblasts were differentiated for 4 days and treated with either DMSO or ARK-0177103 for 24h

Multiple rSMs correct splicing defects in patient-derived myocytes

Clinically relevant splicing recovery at 24 hr in differentiated myocytes

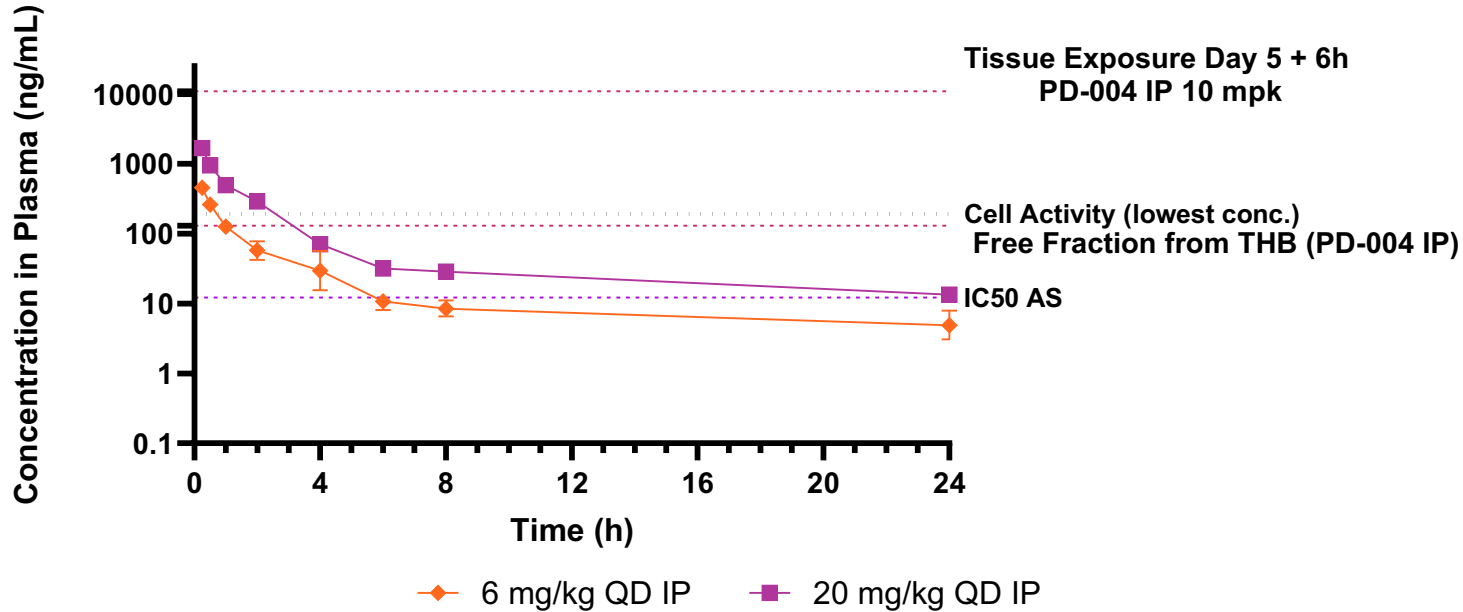


	ARK-178164	ARK-177535
MBNL1 displacement (μM)	0.015	0.019
Splicing in cells (μM)	0.3	0.3
MDCK (Papp x10 ⁻⁶ , cm/s)	0.24	0.09

* DMD, ATP2A, CLASP1, MBNL1 and MBNL2

ARK-177535: High potency, low exposure

ARK177535-002 Mouse PK



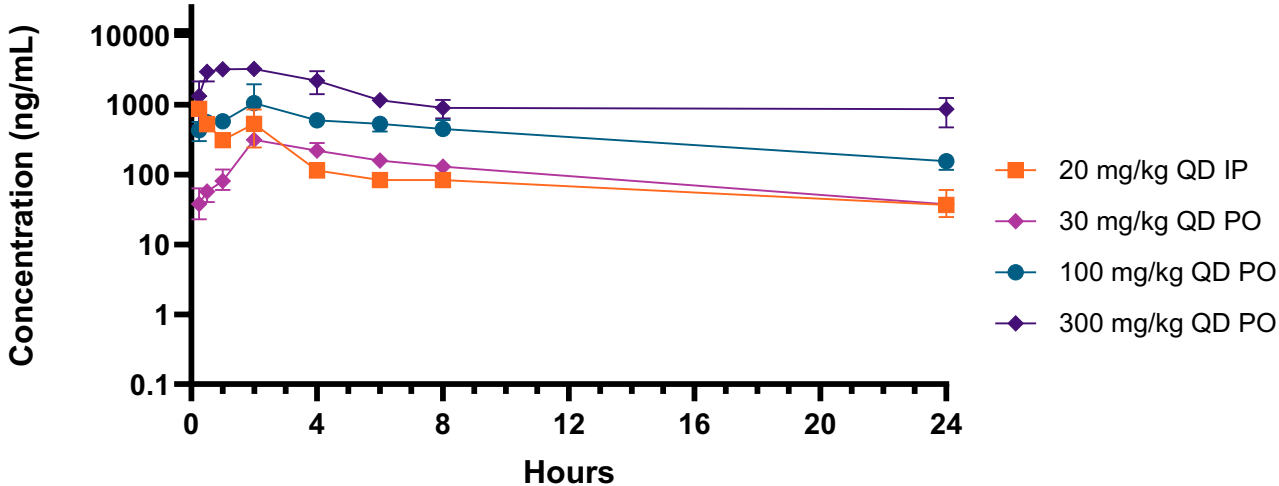
PK parameters	6 mg/kg QD IP	20 mg/kg QD IP
T _{1/2} (h)	12.6	12.8
T _{max} (h)	0.250	0.250
C _{max} (ng/mL)	455	1677
AUC _{last} (h*ng/mL)	588	2150
AUC _{inf} (h*ng/mL)	649	2487
F (%)	51.7	56.4

PK parameters	0.3 mg/kg QD IV
Cl _{obs} (mL/min/kg)	89
V _{ss_obs} (L/kg)	34.2

Dose (mpk)	RoA	Gastroc ng/g	Gastroc μM	Quad ng/g	Quad μM	Brain ng/g	Brain μM	Heart ng/g	Heart μM
6	IP	620	0.97	774	1.21	27.1	0.042	2236	3.48
20	IP	1648	2.57	2272	3.54	71.4	0.11	5032	7.84

ARK-177593: Low potency, high exposure, oral bioavailability

ARK177593 Mouse PK



PK parameters	20 mg/kg QD IP	30 mg/kg QD PO	100 mg/kg QD PO	300 mg/kg QD PO
T _{1/2} (h)	16.9	8.70	9.51	NA
T _{max} (h)	0.250	2.00	4.00	1.17
C _{max} (ng/mL)	878	316	1080	3703
AUC _{last} (h*ng/mL)	2902	2807	9930	30591
AUC _{inf} (h*ng/mL)	4035	3283	11953	NA
F (%)	100	64.5	63.2	62.4

PK parameters	0.3 mg/kg QD IV
Cl _{obs} (mL/min/kg)	87
V _{ss,obs} (L/kg)	56.3

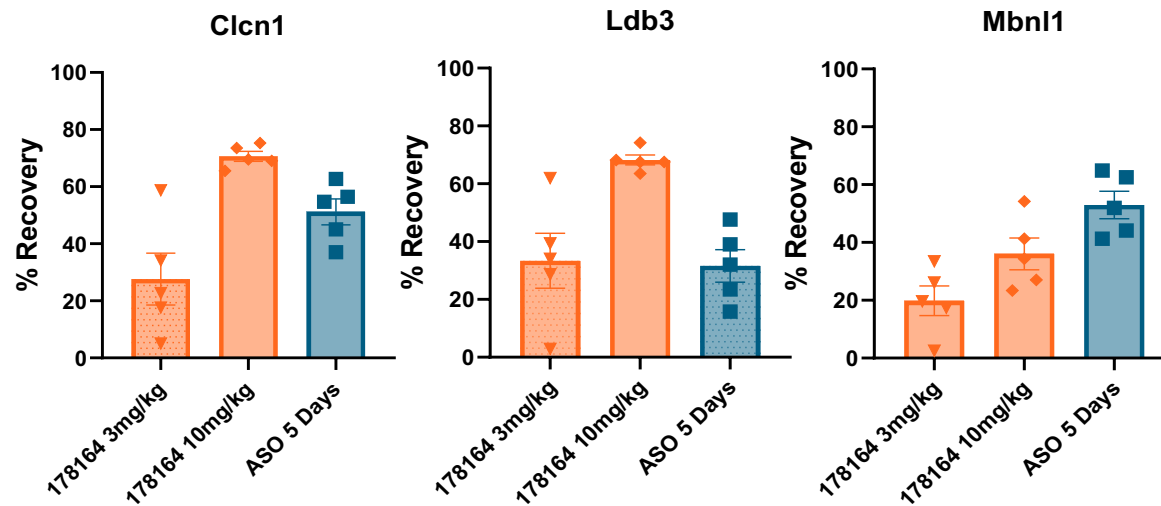
Dose	RoA	Quad ng/g	Quad μM	Heart ng/g	Heart μM
0.3	IV	34.5	0.08	92.2	0.21
20	IP	571	1.30	Not collected	Not collected
30	PO	690	1.57	Not collected	Not collected
100	PO	3814	8.67	6040	13.73
300	PO	15140	34.41	35900	81.59

HSA^{LR} mouse model of myotonic dystrophy

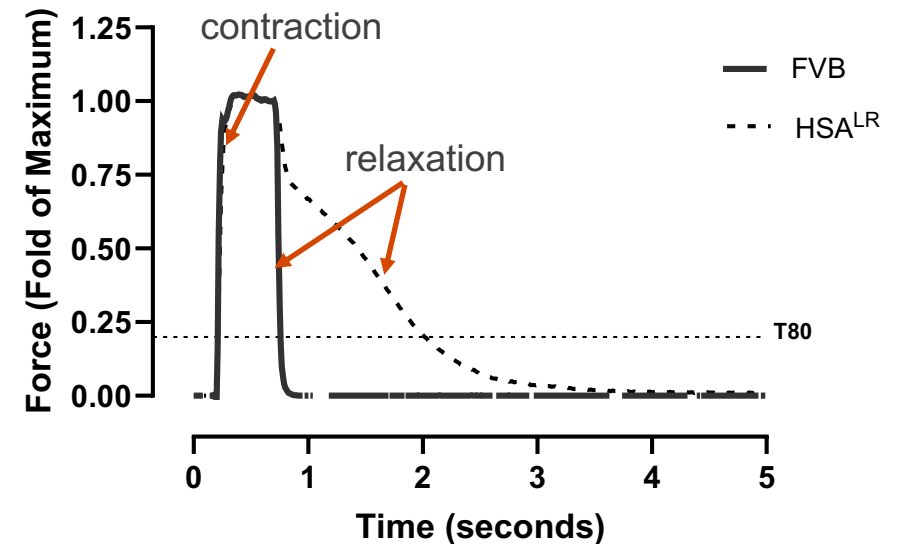
- HSA^{LR} transgenic mice express a human skeletal actin gene (HSA) containing a CTG repeat expansion of approximately 250 repeats⁽¹⁾
- This model shows two hallmarks of the human disease: Splicing defects and myotonia in skeletal muscle



Pharmacodynamics: normalization (recovery) of splicing patterns in panel of clinically relevant genes



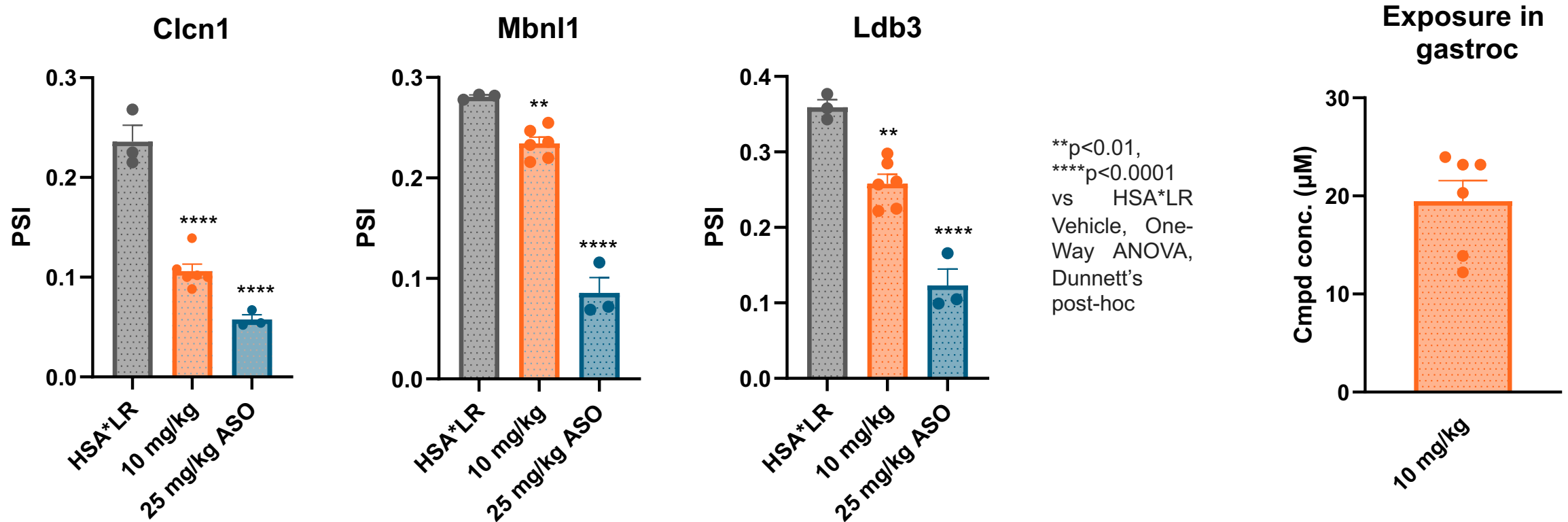
Efficacy: improvement in muscle relaxation after stimulated contraction



Measuring time it takes to reach 80% (T80) of muscle relaxation

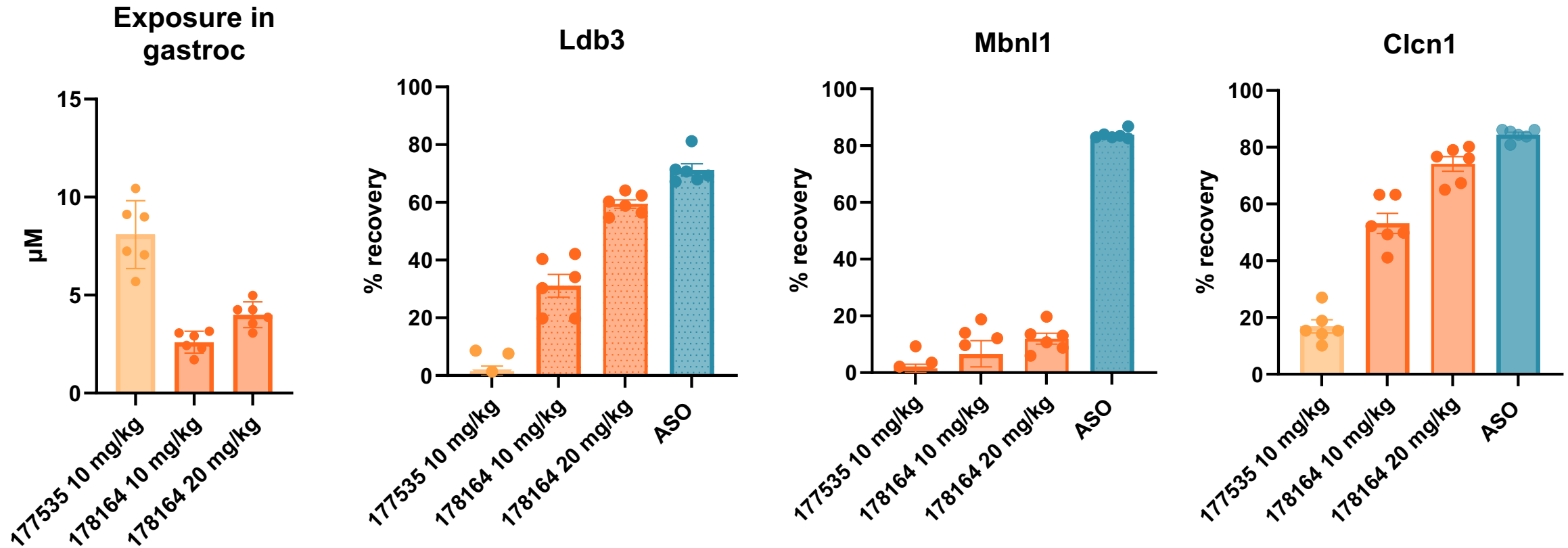
1. A. Mankodi et al, Myotonic Dystrophy in Transgenic Mice Expressing an Expanded CUG Repeat. *Science* **289**, 1769–1772 (2000)

ARK-177535 administered IP modulates multiple relevant splicing events in HSA^{LR} mice



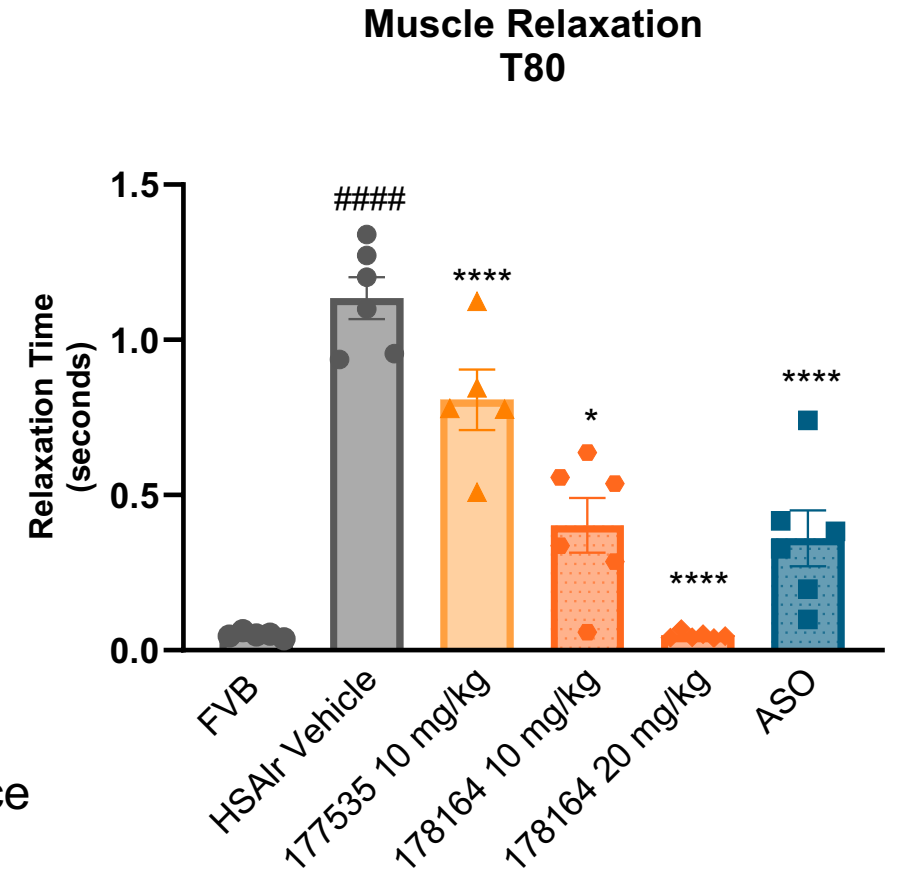
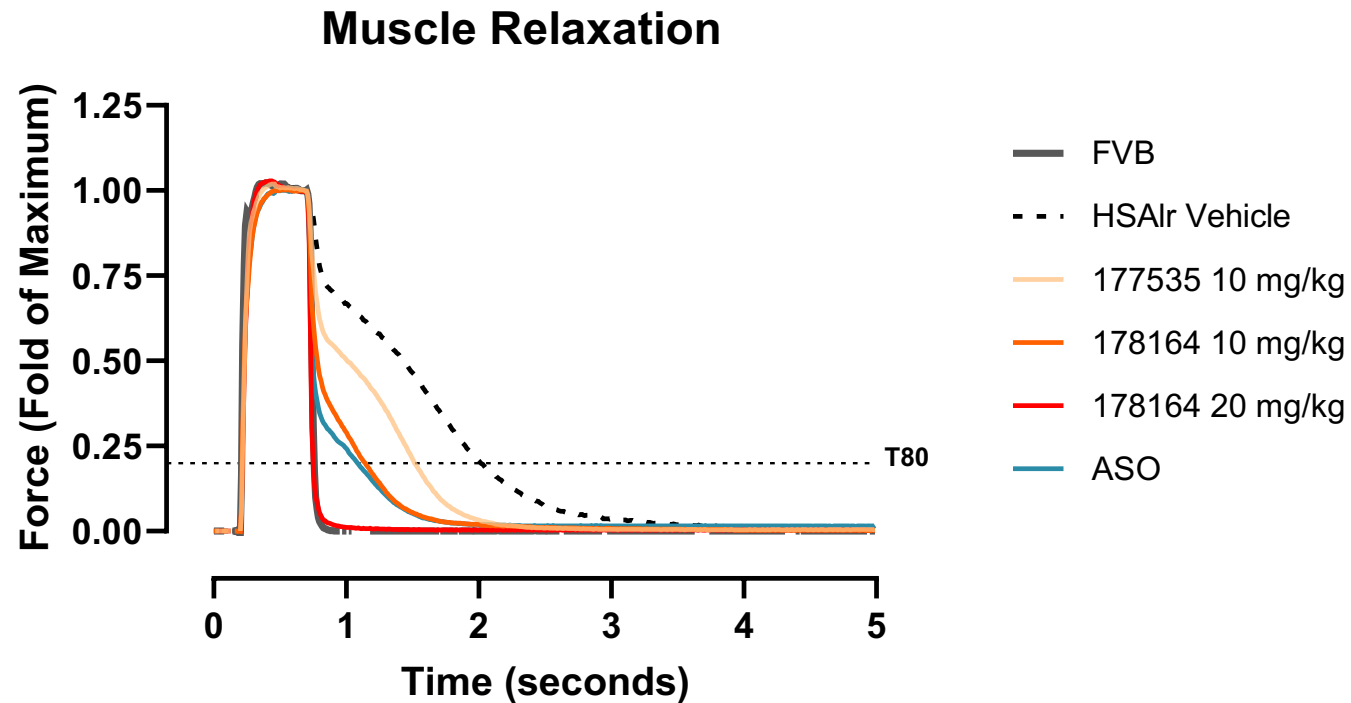
- ARK-177535 is **98.8%** bound in gastroc homogenates, suggesting only ~0.24 μM of free fraction
- Minimal concentration for ARK-177535 to show splicing rescue in human DM1 cells is 0.3 μM
- ASO was injected directly into the gastrocnemius muscle and ARK-177535 administered QD for 5 days IP
- Tissues were analyzed for correction in splicing defects by RNA amplicon seq analysis.

Exposure and PD in muscle tissue via IP administration



ASO was injected directly into the gastrocnemius muscle and ARK-177535 administered QD for 5 days IP. Tissues were analyzed for correction in splicing defects by RNA amplicon seq analysis.

ARK-178164 and ARK-177535 reverse myotonia in HSA^{LR} mice



- Compounds were dosed IP daily for 5 days; ASO control injected once IM in gastrocnemius
- Effect on myotonia was measured 4 hrs after last injection by measuring the time to reach 80% of muscle plantarflexion relaxation (stimulation-induced pressing by the mouse's foot against a machine that measures torque)

$p < 0.001$, vs. FVB vehicle, unpaired t-test of Log-transformed data; * $p < 0.05$, **** $p < 0.0001$ vs HSAIr Vehicle, One-Way ANOVA, Dunnett's post-hoc

Acknowledgments

RNA and Discovery Biology

Craig Blain
Alex Seletsky
Lu Han
Timothy Demers
Stephen Doris
Nabanita De
Jose Saavedra
Haina Huang
Pooja Joshi
Alec Sexton
Helene Chamberlin
Emily Schutsky
Andrew Walker
Lexi Gehring
Lane Anderson
Linda Honaker
Hayden Casassa
Becky Lock
Ewa Stypulkowski
Sarah Mahoney
Wan Yee Leong
Namuun Erdenepurev
Madaline Gilbert
Alyssa Kelly
Amit Shahar
Hunter Linton
Ava Devaney

Molecular Pharmacology

Nick Marsh
Francoise Powell
Ian Wilson
Raphael Bruckner
Carla Neckles
Scott Rusin
Dhruv Bajaj
Scott Gorman
Tony Montibello
Virginia Tsai
Joel Dufour
Gary Frey



Chemical Sciences

Lee Roberts
Elena Menichelli
Karthik Iyer
Herschel Mukherjee
Robin Prince
Yaqiang Wang
Elias Ndaru
Emily Garcia Segal
Charles Perry

Anna Mathias
Jenni Nguyen
Neil Lajkiewicz
Lindsay Chatkewitz
Colin Mizia
Bill Coldren
Anton Filikov
Wilnelly Martinez Ortiz
Sundar Jubilant

Data Sciences

Dave Mauger
Luis Soares
Kimberly Robasky
John Cooper
Lee Vandivier
Carrie Kovalak
Alex Amlie-Wolf
Michael Rutenberg
Schoenberg
Rishab Narula
Jeel Kordiya

Executive Team

Mike Gilman
Jennifer Petter
Kathleen McGinness
Domi Stickens
Heather Lounsbury
James Mutamba